Piezoresistance of *n*-Type Germanium*

H. FRITZSCHE
Department of Physics and Institute for the Study of Metals, University of Chicago, Chicago, Illinois
(Received February 18, 1959)

The change of electrical resistance in uniaxial tension has been measured over the range 6°K to 300°K for several single-crystal specimens of germanium doped with arsenic or antimony. The tensile stress was varied from 1×10^7 to 5×10^8 dynes/cm². Particularly at low temperatures where most of the carriers are bound to impurity centers, the piezoresistance of the conduction band departs strongly from linearity in stress. For the large piezoresistance effects measured with uniaxial stress in [110] direction, these departures depend in size and magnitude on the kind of donor impurity. It is shown that if the strain-induced shift of the Fermi energy is taken into consideration these effects are to be expected from the electron transfer model, which attributes the large piezoresistance to the strain-induced changes of the electron concentrations in the various conduction band valleys. Theoretical predictions concerning the lowest donor states—a one-fold 1*s*-like ground state and a higher lying three-fold state—are verified for As in Ge. The energy separation between these two states is $(4.10\pm0.15)\times10^{-3}$ ev for As and at least by an order of magnitude smaller for Sb in Ge. The deformation potential constant (conduction band) for pure shear strain was found to be $E_2=19.2\pm0.4$ ev at 6.6°K. The mobility anisotropy of a valley was found to decrease with decreasing T because of anisotropic scattering by ionized impurities.

I. INTRODUCTION

THE large effect[1] of elastic shear strain on the electrical resistivity of some multivalley semiconductors has found a very satisfactory explanation in the electron transfer model of Herring[2] and Adams[3] which attributes the effect predominantly to the strain-induced change in the relative populations of the different valleys. Since then the anisotropy of this piezoresistance effect has been employed[4] to determine whether semiconductors are of the multivalley type and, if that is the case, the orientation of their band-edge points. One of the principal predictions of the electron transfer model is that the large components of the piezoresistance matrix depend on the mobility anisotropy characterizing a valley and are proportional to the relative change of the valley populations. Assuming Boltzmann statistics this relative change in population is, for the ith valley, given by

$$\Delta n^{(i)}/n^{(i)}\approx-\epsilon^{(i)}/kT.$$

The energy shift of the valley minima $\epsilon^{(i)}=E_c{}^{(i)}-E_{c0}$ is related to the applied stress through the deformation potential constants.[5]

Except for a small temperature dependence of the mobility anisotropy the theory therefore predicts a $1/T$ dependence of the large piezoresistance components. This has been confirmed between 77° and 380°K by Keyes[6] in *n*-type Ge. More recent experiments[7] at lower temperatures showed, however, deviations from the $1/T$ dependence which varied from sample to sample and which were too large to be accounted for by a temperature dependence of the mobility anisotropy factor. The authors pointed out that this departure from linearity in $1/T$ may be caused partly by inhomogeneities, but they did not offer a satisfactory explanation for the main part of this effect.

The object of the present work is to study more carefully at low temperatures the departure of the piezoresistance from linear dependence on the applied stress and to test the predictions of the electron transfer model at large stresses. Terms of higher order in stress are to be expected when the condition $|\epsilon^{(i)}|/kT\ll1$ ceases to be fulfilled and the power expansion of the Boltzmann factor is no longer permissible. Assuming a deformation potential $E_2\approx19$ ev for *n*-type Ge, one obtains $\epsilon^{(i)}/kT=5.1\times10^{-8}X/T$ for uniaxial stress X[dyne/cm²] in the [110] direction [see Eq. (A5) of Appendix]. Hence this ratio becomes of the order of unity at moderate stresses of 2×10^8 dyne/cm² at around 10°K so that terms of higher order in stress should become noticeable.

Reported below are measurements at temperatures between 300°K and 6°K of the piezoresistance effect of germanium doped with As and with Sb using uniaxial tensile stresses ranging from 1×10^7 to 4.5×10^8 dyne/cm². The results will be compared with expressions which are derived from the electron transfer model taking into account the stress-induced changes of the Fermi level and of the impurity activation energy.

II. EXPERIMENTAL DETAILS

In the limit of small stresses the stress-induced change of the conductivity tensor $\boldsymbol{\sigma}$ is related to the stress tensor $\mathbf{X}$ by[8]

$$(\Delta\sigma/\sigma_0)_r=\sum_s \Pi_{rs}X_s. \quad (1)$$

* This work was supported in part by the National Science Foundation and the U. S. Atomic Energy Commission.

[1] C. S. Smith, Phys. Rev. **94**, 42 (1954).
[2] C. Herring, Bell System Tech. J. **34**, 237 (1955).
[3] E. N. Adams, Chicago Midway Laboratories Technical Report CML-TN-P3 (unpublished).
[4] R. F. Potter, Phys. Rev. **108**, 652 (1957); A. J. Tuzzolino, Phys. Rev. **109**, 1980 (1958); **112**, 30 (1958). A. Sagar, Phys. Rev. **112**, 1533 (1958).
[5] C. Herring and E. Vogt, Phys. Rev. **101**, 944 (1956).
[6] R. W. Keyes, Phys. Rev. **100**, 1104 (1955).
[7] Morin, Geballe, and Herring, Phys. Rev. **105**, 525 (1957).
[8] The piezoresistance coefficients were taken to be positive when tensile stress increased the conductivity. Thus, our coefficients are opposite in sign to those of Smith (reference 1).

Here the subscripts r and s are the abbreviated suffices customary in elasticity theory and run from 1 to 6. In the case of cubic crystals one usually chooses the 11, 12 and 44 components referred to coordinate axes parallel to the cube axes as the three independent components of the piezoresistance matrix **II**.

As discussed by Smith,[1] three measurements with different crystallographic orientations of the current and stress system are necessary to determine the three piezoresistance constants. Table I lists various arrangements which were used for this purpose by Smith and also in this work. The combination of Π_{rs} determined in each case[8] is listed in the fourth column of Table I.

At larger values of applied stress, or more accurately at larger values of the ratio X/T, the linear relation (1) ceases to hold and a larger number of different orientations have to be investigated to determine all parameters necessary for the description of the piezoresistance effect.

TABLE I. Piezoresistance coefficients for various arrangements of X and I.

Orientation Stress X	Orientation Current I	Arrangement	$\frac{\Delta\sigma}{\sigma_0 X}\Big\vert_{X\to 0}$
[100]	[100]	A	Π_{11}
[100]	[010]	B	Π_{12}
[110]	[110]	C	$(\Pi_{11}+\Pi_{12}+\Pi_{44})/2$
[110]	[1$\bar{1}$0]	D	$(\Pi_{11}+\Pi_{12}-\Pi_{44})/2$

(i) Specimens and Their Preparation

All samples were single crystals, oriented by x-rays to better than one degree, and then cut perpendicular to the growth axis to minimize the impurity concentration gradient along their length. They were rectangular bars of approximately 0.01 cm^2 cross section and 2.5 cm length. All surfaces were etched. The dislocation density was determined by etch-pit counts on a (111) face and the donor and acceptor concencentrations, N_d and N_a, respectively, by Hall measurements. The characteristics of the samples[9] are listed in Table II.

TABLE II. Sample characteristics.

Sample No.	$N_d\times10^{-15}$ (cm^{-3})	$N_a\times10^{-15}$ (cm^{-3})	Dislocation density (cm^{-2})
As-1	7.8	0.37	1.5×10^4
As-2	35	2.3	2×10^3
As-3	36	2.3	2×10^3
Sb-4	5.0	0.24	3×10^3

Details of the mounting of the sample are shown in Fig. 1. For measuring the longitudinal piezoresistance six leads were attached by soldering No. 38 copper wires to the samples with Sn-In solder. The two pairs of potential leads enable one to check the homogeneity of the stress distribution. Beyond a distance of about 0.3 cm from the attached brass cups (see Fig. 1), good homogeneity was ascertained. For the transverse piezoresistance measurements, a 20–30 micron thick and 0.5 cm long layer of Sn-In solder was applied on opposite and previously etched faces near the center of the sample. One copper wire was soldered to each of the large-area electrodes and the sample was then subjected to a final etch to eliminate the danger of surface conduction.

The voltages were measured with a conventional dc potentiometer circuit using a galvanometer or a vibrating reed electrometer as a zero-indicating instrument. The contacts were always found to be ohmic. The electric field was kept low enough so that the resistivity and the piezoresistance effect were independent of the field.

(ii) The Apparatus

The cryostat used for maintaining temperatures in the range 7° to 300°K is of conventional design. Helium was used as refrigerant. The sample was inside a heavy copper can which also contained charcoal saturated with adsorbed helium to increase the heat capacity. Thermal control was achieved by means of a heater wound around the copper can and, if necessary, by slowly desorbing the adsorbed helium from the charcoal.[10] The temperature was measured with a 0.1-watt Allen-Bradley carbon resistor placed inside the copper can in close proximity to the sample.

About 0.4 cm of each end of the germanium samples were cemented into closely fitting brass cups with red sealing wax (see Fig. 1). Two strings 1.5 cm long were attached to these cups and served as electrical insulation and as means for avoiding torsional strains in the sample. One of these strings was rigidly fixed at the bottom of the sample holder frame. The other was attached to the lower end of a thin stainless steel tube which in turn hung from the short lever of a beam balance. The balance itself was inside a vacuum-tight enclosure. A set of weights could be attached to its

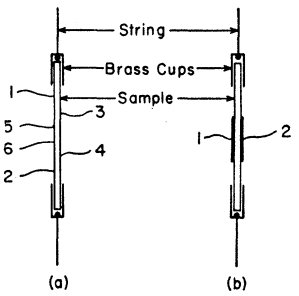

FIG. 1. Mounting of samples and arrangement of electrodes for a longitudinal case (a) and a transverse case (b). In case (a) the wires 1 and 2 serve as current electrodes and 3 to 6 as two pairs of potential electrodes. In case (b) the potential difference is measured directly between the current electrodes 1 and 2.

[9] Sample As-1 was cut from a crystal which was kindly supplied by Dr. N. B. Hannay of the Bell Telephone Laboratories.

[10] A. C. Rose-Innes and R. F. Broom, J. Sci. Instr. **33**, 31 (1956).

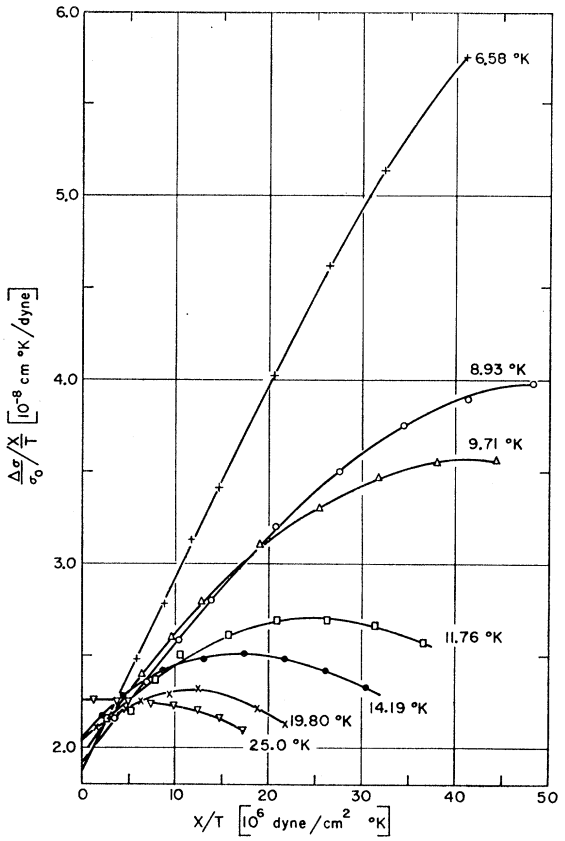

FIG. 2. $(\Delta\sigma/\sigma_0)/(X/T)$ as a function of X/T for As-doped germanium in arrangement C at various temperatures. The curve $T=6.58$°K was measured on sample As-1, the others on sample As-2. The intercepts with the ordinate yield $T(\Pi_{11}+\Pi_{12}+\Pi_{44})/2$.

long lever arm. The largest tensile stress applied was kept at 5×10^8 dynes/cm² to avoid breakage. Sufficient time was allowed for the sample to reach thermal equilibrium after each change of load.

(iii) Internal Strains in the Absence of Applied Stress

Depending on the conditions under which the crystals were grown, considerable strains may be frozen in the material. Assuming a relationship[11] between these internal stresses, τ_{int}, and the number of dislocation lines per cm², n, the approximate magnitude of the τ_{int} can be estimated from the known stress field around a dislocation.[12] Halfway between the dislocations the stress is approximately $\tau_{\text{int}}\approx3\times10^3(n)^{\frac{1}{2}}$ dyne/cm. For the largest dislocation densities found in our samples (see Table II), this estimate yields $\tau_{\text{int}}\approx4\times10^5$ dyne/cm² which is smaller than the smallest stress applied.

More serious, however, is the strain due to the different thermal expansion of germanium and the solder near the large-area contacts of the transverse arrangements. Although the thickness of the solder layer was mostly kept below 30 microns, small errors may have been caused by this effect.

III. RESULTS AND DISCUSSION

Most of the results discussed below have been checked for reproducibility using different samples, changing the sample mounting and the arrangement of electrodes, and investigating the effect of small misalignments.

In order to determine accurately the small-stress limit of the piezoresistance effect, the experimental results will be presented by plots of $(\Delta\sigma/\sigma_0)/(X/T)$ *versus* X/T. Figure 2 shows the large longitudinal effect

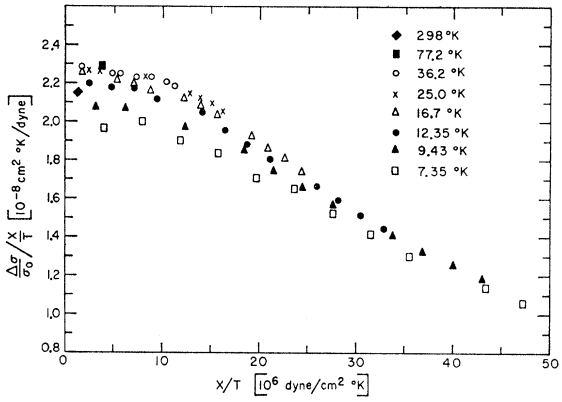

FIG. 3. $(\Delta\sigma/\sigma_0)/(X/T)$ as a function of X/T for Sb-doped germanium (sample Sb-4) in arrangement C. The intercepts with the ordinate yield $T(\Pi_{11}+\Pi_{12}+\Pi_{44})/2$.

(arrangement C) for As-doped germanium. The various curves were obtained at different temperatures as indicated in the figure. In the exhaustion range the curves decrease slightly at large values of X/T. But as soon as the temperature becomes low enough for carriers to freeze into the donor states, large deviations from the linear relationship of Eq. (1) become evident. The largest deviations are found at the lowest temperatures where $(\Delta\sigma/\sigma_0)/(X/T)$ increases to almost three times its small-stress limit.

The corresponding measurement on Sb-doped germanium are presented in Fig. 3. Here the behavior of the piezoresistance effect at large stresses is completely different. Even at the lowest temperatures $(\Delta\sigma/\sigma_0)/(X/T)$ decreases with increasing X/T and the curves measured at various T appear to be remarkably similar. A comparison of Figs. 2 and 3 demonstrates how the terms of higher order in the stress depend on the nature of the donor impurity. This is despite the fact that

[11] S. Lederhandler finds a correlation between the density of dislocations and the internal stress deduced from the birefringence pattern in Si which seems to support the relation used above (private communication); see also S. Lederhandler, Bull. Am. Phys. Soc. 3, 358 (1958).

[12] W. T. Read, *Dislocations in Crystals* (McGraw-Hill Book Company, New York, 1953).

conduction takes place in the conduction band only. As shown below, impurity conduction sets in at much lower temperature.

The small piezoresistance effects (arrangements A and B) of As-doped germanium are shown in Figs. 4 and 5, respectively. Although these measurements are less accurate because of the smallness of the conductivity change, considerable deviations from the linear stress dependence become noticeable at the lower temperatures. However, even at large stresses the piezoresistance effect of these orientations remains small in comparison with that of arrangement C.

Low-Stress Limit of the Piezoresistance

In order to obtain the correct piezoresistance terms of first order in X, the curves of Figs. 2, 4, and 5 and of a similar plot obtained with As-doped germanium in arrangement D were extrapolated to the axis $X/T=0$. The appropriate corrections were applied as discussed by Smith[1] to account for the dimensional changes and for the fact that the current lines are not straight at the ends of the electrodes in the transverse cases B and D. These corrected quantities are plotted against $1/T$ in Fig. 6. They represent the product of temperature with the appropriate combination of piezoresistance coefficients as indicated. It was convenient to change the sign of the results obtained with arrangement D, the only one which yields negative conductivity changes.

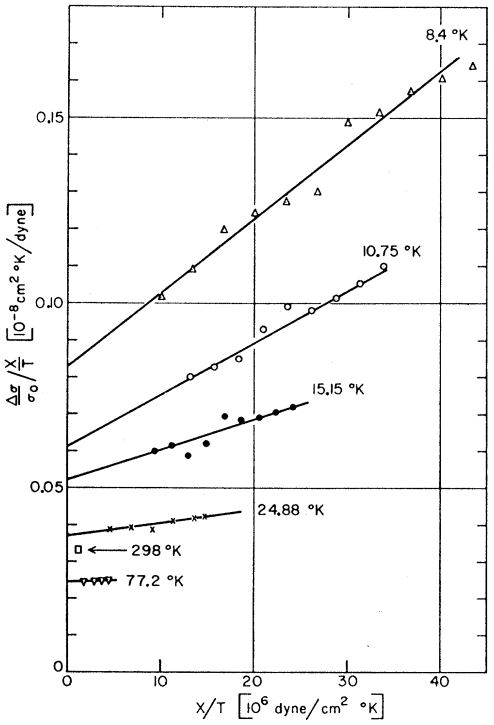

FIG. 4. $(\Delta\sigma/\sigma_0)/(X/T)$ as a function of X/T for As-doped germanium (As-3) in arrangement A. The intercepts yield $T\Pi_{11}$.

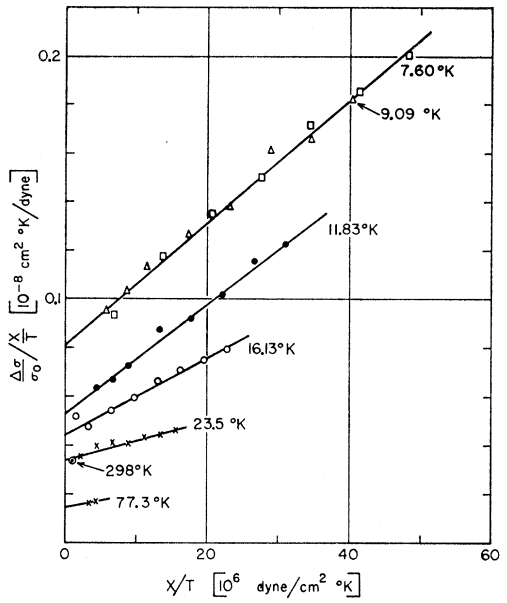

FIG. 5. $(\Delta\sigma/\sigma_0)/(X/T)$ as a function of X/T for As-doped germanium (As-3) in arrangement B. The intercepts yield $T\Pi_{12}$.

In the whole temperature range, the coefficients Π_{11} and Π_{12} are much smaller than Π_{44}, in agreement with previous measurements.[1,7] Possible causes for the finite values of the small coefficients Π_{11} and Π_{12} have been discussed by Morin, Geballe, and Herring[7] and no further information can be added at present.

The quantities presented in Fig. 6 are not quite consistent with one another. One obtains somewhat different values for Π_{44} depending on whether it is determined from curves A, B, and C, from curves A, B, and D, or from the two curves C and D. One of the reasons for this discrepancy is believed due to the uncertainty involved in the rather large end corrections[13] which have to be made in the transverse cases as mentioned above. In the case of arrangement D this correction is up to four times larger than the small effects measured with arrangements A and B. The values for $\frac{1}{2}T\Pi_{44}$ obtained from curves A, B, and C were, therefore, considered more accurate. They are represented by the dotted curve in Fig. 6.

Discussion of Π_{44}

Theory predicts that the predominant contributions to Π_{44} in n-type germanium come from the strain-

[13] In deriving the correction formula (see reference 1) which accounts for the distortion of the current lines at the ends of the electrodes in the transverse case, H. Suhl assumed the resistance of the electrodes to be negligible compared to the resistance of the sample. Because of the small thickness of our large-area contacts, this assumption is not justified above 15°K where the sample resistance is low. Hence the effective length of the electrodes is decreased and a correspondingly larger end correction should be applied. This might be the reason for the rather large discrepancy between the Π_{44}'s calculated from arrangement C and D at temperatures above 15°K.

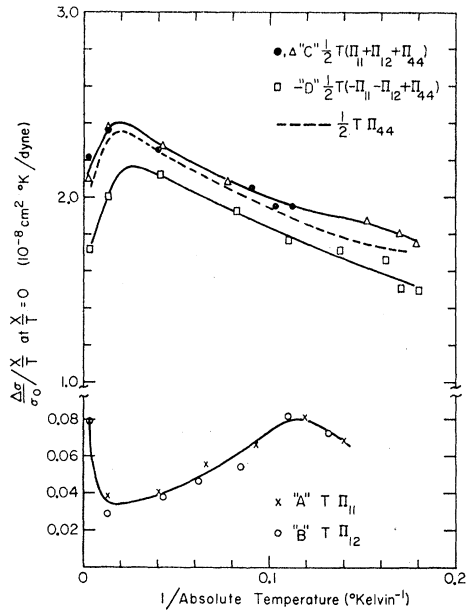

FIG. 6. The intercepts of the curves of Figs. 1, 3, and 4 with the ordinate $X/T=0$ as a function of reciprocal temperature. These values have been corrected for dimensional changes and the end effects occurring at the transverse electrodes (see text). The sign of the values obtained for arrangement D has been changed to positive. The full circles are data obtained with As-2, the triangles those obtained with As-1. The dotted curve represents $T\Pi_{44}/2$ as calculated from curves A, B, and C.

induced change in the relative populations of the different valleys. This leads to the expression [see Eq. (A14) of Appendix]

$$\Pi_{44}=-\frac{1}{3}\frac{E_2}{kT}S_{44}\frac{K-1}{2K+1}, \tag{2}$$

where E_2 is the deformation potential constant for pure shear, S_{44} is the elastic constant, and $K=\mu_1/\mu_{11}$ is the mobility anisotropy of a valley. A temperature dependence of the product $T\Pi_{44}$ can arise from a change of K or of E_2 with temperature. The temperature dependence of S_{44} is negligible. Magnetoresistance measurements[14,15] have shown that one can expect a decrease of K from its pure-lattice-scattering value $K\approx 20$ to values of the order of unity for ionized-impurity scattering as the temperature is lowered. While this can account for the observed decrease of $\frac{1}{2}T\Pi_{44}$ between 50°K and 7°K, it cannot explain the sudden decrease as the temperature is raised from 77°K to 300°K (see Fig. 6). This latter decrease is attributed to a small negative temperature-independent contribution to Π_{44} which arises from (a) the minor effects which are also responsible for the finite values of Π_{11} and Π_{12} and (b) from the temperature-dependent term in the deformation potential which may be written as $E_2=E_2^0(1+\alpha T)$. This temperature-independent contribution[16] to Π_{44} will be denoted by Π_{44}'. It is negligibly small compared with Π_{44} at low temperatures; its presence becomes noticeable only at high temperatures where Π_{44} is small.

In the next section a value of $E_2=19.2$ ev will be derived from the terms in the piezoresistance of higher order in stress. Using this value for E_2, the temperature dependence of K shown in Fig. 7 could be obtained from the $\frac{1}{2}T\Pi_{44}$ curve below 50°K (see Fig. 6). This decrease of K with temperature agrees qualitatively with the results of the magnetoresistance measurements.[14,15] We found no indication of a subsequent increase of K like that observed by Laff and Fan[15] around 6°K which they attributed to neutral-impurity scattering.

The *K versus T* curve of Fig. 7 was extrapolated to higher temperatures (dotted part) in accordance with the results of the magnetoresistance measurements. Using these values for K, the value of $\Pi_{44}'=-16\times10^{-12}$ cm²/dyne was obtained as the best fit to the high-

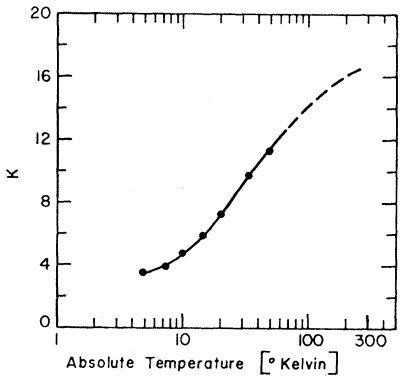

FIG. 7. The mobility anisotropy $K=\mu_1/\mu_{11}$ of a valley as a function of temperature for As-1 and As-2.

temperature part of the $\frac{1}{2}T\Pi_{44}$ curve in Fig. 6. If a temperature variation of E_2 were the only cause for the occurrence of Π_{44}', one would obtain for the temperature coefficient $\alpha\approx-6\times10^{-4}$/°K.

In order to show that the piezoresistance coefficients plotted in Fig. 6 have not been influenced by small admixtures of impurity conduction, the temperature dependence of the zero-strain resistivity ρ_0 and of the low-stress limit of $\Delta\sigma/\sigma_0$ is shown for a typical case in Fig. 8. Near the onset of impurity conduction, $\Delta\sigma/\sigma_0$ reaches a maximum and falls off very rapidly at lower T. We conclude from this that at temperatures slightly above the maximum the influence of impurity conduction on the results is negligible. As discussed above, the low-stress piezoresistance of the conduction band deviates from a simple $1/T$ law because of the tem-

[14] C. Goldberg, Phys. Rev. **109**, 331 (1958); C. Goldberg and W. E. Howard, Phys. Rev. **110**, 1035 (1958).

[15] R. A. Laff and H. Y. Fan, Phys. Rev. **112**, 317 (1958).

[16] The temperature-independent Π_{44}' is equivalent in meaning and magnitude with the intercept at $1/T=0$ of the straight line fitted by Morin, Geballe, and Herring to their $\Delta\rho/\rho X$ *versus* $1/T$ plots. See Fig. 4 of reference 7.

perature dependence of K. The term Π_{44}' gives rise to a very small vertical shift of the curve.

Piezoresistance at Large Stresses

The different character of the piezoresistance of germanium doped with As (Fig. 2) and doped with Sb (Fig. 3) demonstrates that it is necessary to consider the detailed structure of the lowest donor levels in calculating the conductivity change at large stresses.

In the Appendix expressions for the conductivity changes are derived for two extreme cases: $\Delta_c=0$ (case I) and $4\Delta_c \gg kT$ (case II). $4\Delta_c$ is the magnitude of the energy separation between the one-fold and the three-fold 1s-like donor states in unstrained germanium.[17,18] The order of magnitude of Δ_c can be estimated[17,18a] for a particular donor by comparing the observed donor activation energy, E_{obs}, obtained from Hall measure-

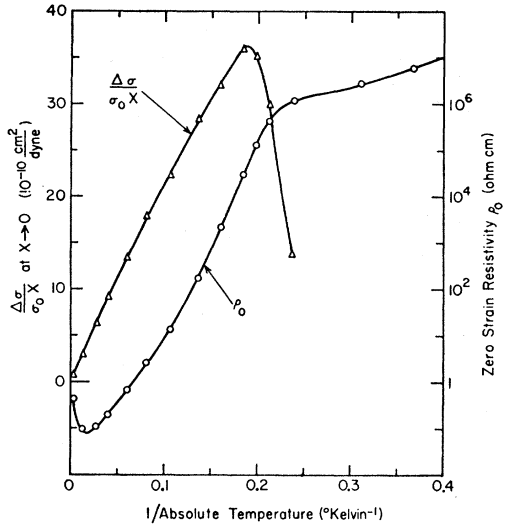

FIG. 8. Zero-strain resistivity and the low-stress limit of the piezoresistance as a function of reciprocal temperature for Sb-doped germanium (Sb-4) in arrangement C.

ments with that calculated from the effective-mass formalism, $E_{\text{eff.mass}}$. Since the three-fold donor state is least affected by the corrections to the effective-mass formalism, one can set

$$4\Delta_c \approx E_{\text{obs}} - E_{\text{eff.mass}}.$$

This yields for Sb in germanium $4\Delta_c \approx 4\times10^{-4}$ ev and for As in germanium $4\Delta_c \approx 3.5\times10^{-3}$ ev.

For the Sb-doped samples, $\Delta_c/kT \ll 1$ for temperatures which are not too low, so that the expressions derived for case I should be good approximations. Figure 9 shows a comparison of the Sb results with Eq. (A13). For the As-doped samples, the condition

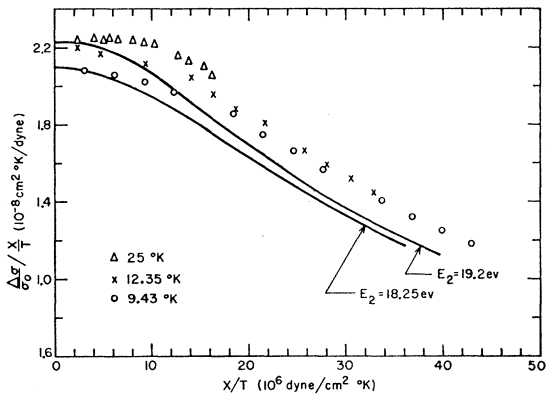

FIG. 9. Comparison of the piezoresistance effect measured on Sb-doped germanium in arrangement C with theoretical curves obtained from Eq. (A13) using two different deformation potentials E_2. A different choice of the mobility anisotropy K causes a vertical shift of the theoretical curves.

$4\Delta_c/kT \gg 1$ for case II is fairly well satisfied at the lowest temperatures. In Fig. 10, curves calculated from Eq. (A16) are compared with experimental results obtained at $T=6.58$°K and $T=8.93$°K with As-doped germanium. In order to calculate the theoretical curves, the values of E_2, Δ_c, and $(K-1)/(2K+1)$ have to be known. They were determined in the following way.

Assuming that the initial slope of the $T=6.58$°K curve in Fig. 10 is not influenced by any other effect but the electron transfer mechanism, this slope can be set equal to the coefficient of the quadratic term of the appropriate power expansion of Eq. (A16):

$$\text{slope}=\left(\frac{S_{44}E_2}{6k}\right)^2\left(\frac{1}{2}-\frac{kT}{4\Delta_c}\right). \tag{3}$$

In the curves of Fig. 10 one first subtracts the small term $T(\Pi_{11}+\Pi_{12})/2$ from the intercepts at $X/T=0$.

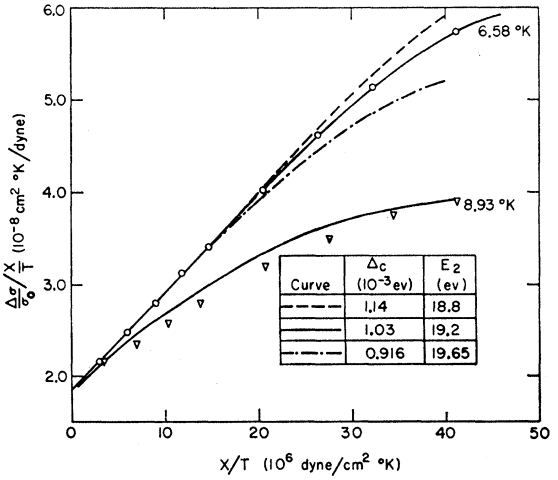

FIG. 10. Comparison of the piezoresistance effect measured on As-doped germanium in arrangement C with theoretical curves calculated from Eq. (A16) for various sets of Δ_c and E_2.

[17] W. Kohn, in *Solid State Physics* edited by F. Seitz and D. Turnbull (Academic Press, Inc., New York, 1957), Vol. 5, p. 257.
[18] P. J. Price, Phys. Rev. **104**, 1223 (1956).
[18a] E. M. Conwell, Phys. Rev. **99**, 1195 (1955).

After this correction the intercepts yield, according to Eq. (2),

$$\tfrac{1}{2}T\Pi_{44}=\frac{1}{6k}E_2S_{44}\frac{K-1}{2K+1}. \quad (4)$$

The two Eqs. (3) and (4) do not suffice to determine the three unknown quantities E_2, Δ_c, and K. These were therefore determined by finding a set of E_2, Δ_c, and K which satisfies (3) and (4) and which simultaneously gives the best fit of the complete expression (A16) to the experimental points. Figure 10 shows the calculated curves for various choices of E_2 and Δ_c together with the experimental points. The best fit was obtained with $E_2=19.2$ ev, $\Delta_c=1.03\times10^{-3}$ ev, and the values of K shown in Fig. 7.

In order to estimate the limits of accuracy for these values, let us briefly examine the assumptions underlying these calculations. In deriving (A16) it was assumed (a) that the total carrier concentration $n\ll N_a$ and $n\ll N_d-N_a$, and (b) that the presence of the higher lying states of the donor multiplet can be neglected. Solving the Fermi level Eq. (A8) with the complete expression (A9) for case II shows that the errors introduced by assumptions (a) and (b) caused the calculated curves of Fig. 10 to be too high by about 0.3% at $T=6.58$°K and by about 2% at 8.93°K. In comparing the observed piezoresistance at large stresses with Eq. (A16), it was furthermore assumed that there are no contributions to the higher order terms in the piezoresistance from the minor effects which are responsible for the finite values observed in arrangements A and B. It seems reasonable to assume that these minor effects add to the results of arrangement C a contribution of equal magnitude as that found in arrangements A and B. The slopes of the curves in Figs. 4 and 5 at the lowest temperatures are about 3% of those in Fig. 10, so that a comparison of the latter with (A16) has to be considered uncertain by this amount.

These considerations combined with an experimental error of about 1% lead to an uncertainty of 4% in Δ_c and of 2% in E_2. The discrepancy between the experimental points and the calculated curve at $T=8.93$°K (see Fig. 10) falls within this margin of errors.

The results obtained at the lowest temperatures with As-doped germanium with stress and current in arrangement D agree qualitatively with the expression (A16) derived in the Appendix for case II. $(\Delta\sigma/\sigma_0)/(X/T)$ is negative at $X/T=0$; it then increases with increasing X/T and assumes positive values at large X/T. We have refrained from a quantitative comparison, however, since in the X/T range where the absolute magnitude of $(\Delta\sigma/\sigma_0)/(X/T)$ is small it will be strongly affected by small additional piezoresistance contributions. These additional contributions are unknown. They cannot be inferred from measurements on arrangements A and B as was the case in the small-stress limit.

The comparison of the Sb results with Eq. (A13) (Fig. 9) shows that the experimental curves do not decrease quite as strongly as the theoretical curve. For the low-temperature curves this may be partly accounted for by assuming a small splitting parameter $\Delta_c\approx10^{-4}$ ev. At higher temperatures such a small splitting should, however, have no effect. A choice of a smaller value for E_2 would yield a better fit at intermediate X/T but a poorer fit at large X/T. Although this discrepancy remains unexplained at present, we feel that the qualitative agreement justifies some confidence in the validity of the model used.

Morin, Geballe, and Herring[7] found at 10°K a negligibly small effect of stress on the carrier concentration in Sb-doped Ge. As shown in the Appendix this is to be expected for $\Delta_c\ll kT$ which seems to be the case for Sb in Ge. For As in Ge, on the other hand, the low-temperature Hall coefficient should change considerably according to Eq. (A17) of the Appendix.

Recently Weinreich[19] discussed the possibility that the three-fold 1s-like donor state in unstrained germanium is the ground state and that the onefold state lies higher by $4\Delta_c$. This amounts to turning the donor state multiplet of Fig. 11(b) upside down and using a Δ_c of opposite sign in Eqs. (A7). We have calculated the expression for the piezoresistance using the inverted model of Weinreich and found it impossible to explain the results on As-doped germanium with his model.

IV. CONCLUSIONS

These experiments indicate that the electron transfer model forms an excellent basis for the understanding of the large piezoresistance effects in germanium. An analysis of the piezoresistance as a function of stress can yield information concerning the nature of the lowest lying impurity states.

The results on As-doped germanium confirm the theoretical predictions of a onefold 1s-like donor ground state and an energy gap between the next higher lying threefold state and the ground state of about $4\Delta_c=(4.10\pm0.15)\times10^{-3}$ ev for As. This energy gap is smaller by an order of magnitude for Sb.

In the case of a multivalley semiconductor containing impurities, whose ground states are almost unaffected by strain, the deformation potential E_2 can be determined from the term in $\Delta\sigma/\sigma_0$ which is quadratic in stress using suitable orientations for current and stress. This method has the advantage of being independent of the temperature-dependent mobility anisotropy of a valley. The deformation potential for electrons in germanium at low temperatures was determined in this way as $E_2^0=(19.2\pm0.4)$ ev with As as donor impurities.

[19] Weinreich, Boyle, White, and Rodgers, Phys. Rev. Letters 2, 96 (1959).

Previous estimates[5,20] of the deformation potential near room temperature yielded a value of $E_2 \approx 16$ ev. The apparent disagreement between these values disappears if one assumes a temperature dependence of approximately $E_2 = E_2^0(1-6\times10^{-4}T)$. Our results, particularly the presence of the additional constant term Π_{44}', are compatible with a temperature dependence of E_2 of this magnitude. They do not suffice, however, to establish it because of the various other factors which might contribute to Π_{44}'.

ACKNOWLEDGMENTS

I am indebted to Mr. Ramon Hoff for the preparation of some of the germanium crystals, for the x-ray orientations, and for the determination of dislocation densities. I wish to thank Dr. N. B. Hannay of the Bell Telephone Laboratories for providing some germanium crystals used for this investigation.

APPENDIX. PIEZORESISTANCE TO HIGHER ORDERS IN STRAIN

We shall try to extend the expressions obtained by Herring[2] and Adams[3] for the strain-induced change of the electrical conductivity to higher orders in the strain. The discussion will be limited to n-type germanium, the specific case of interest in this paper. This treatment is based on basically the same assumptions as are the calculations of the authors mentioned above:

(a) neglect of the effect of strain on the mobility and on the mobility anisotropy of a valley;

(b) Maxwell-Boltzmann statistics for the carriers in the conduction band;

(c) semiconductor in the extrinsic range.

The only effect of strain considered is a change of the valley populations. The relative change in conductivity is then

$$\frac{\Delta\sigma_{\alpha\beta}}{\sigma_0}=\frac{1}{\mu}\left\langle\frac{\Delta n^{(i)}}{n_0^{(i)}}\mu_{\alpha\beta}^{(i)}\right\rangle_i, \tag{A1}$$

where $\sigma_{\alpha\beta}$ and $\mu_{\alpha\beta}^{(i)}$ are, respectively, components of the total conductivity tensor and of the mobility tensor of the ith valley, both of course referred to the same coordinate system. The angular brackets with subscript i mean that the quantity in brackets should be averaged over all valleys i. The macroscopic mobility $\mu=(\mu_{11}+2\mu_\perp)/3$ depends on μ_{11} and $\mu_\perp$, the mobilities of electrons parallel and perpendicular, respectively, to the axis of revolution of a valley.

With assumption (b) one obtains

$$\frac{\Delta n^{(i)}}{n_0^{(i)}}=\exp[(\epsilon_F-\epsilon^{(i)})/kT]-1, \tag{A2}$$

where $\epsilon^{(i)}=E_c^{(i)}-E_{c0}$ denotes the strain-induced energy shift of the ith valley and $\epsilon_F=E_F-E_{F0}$ the strain-induced shift of the Fermi energy. Expressing $\mu_{\alpha\beta}^{(i)}$ in terms of μ_{11} and $\mu_\perp$ and substituting (A2) in (A1), one can write

$$\frac{\Delta\sigma_{\alpha\beta}}{\sigma_0}=\frac{3}{2\mu_\perp+\mu_{11}}\langle[\exp[(\epsilon_F-\epsilon^{(i)})/kT]-1]\times[\delta_{\alpha\beta}\mu_\perp+n_\alpha^{(i)}n_\beta^{(i)}(\mu_{11}-\mu_\perp)]\rangle_i, \tag{A3}$$

where $\delta_{\alpha\beta}$ is the Kronecker delta and $n_\alpha^{(i)}$, $n_\beta^{(i)}$ are components of $\hat{n}^{(i)}$, the unit vector in the direction of the ith valley in momentum space.

Even for large strains, the linear relation between $\epsilon^{(i)}$ and the strain $\mathbf{u}$ will be assumed to hold as given by the deformation potential theory[5,21]:

$$\epsilon^{(i)}=\hat{n}^{(i)}\cdot\{E_1\,\mathrm{Tr}\mathbf{u}\mathbf{1}+E_2(\mathbf{u}-\tfrac{1}{3}\,\mathrm{Tr}\mathbf{u}\mathbf{1})\}\cdot\hat{n}^{(i)}. \tag{A4}$$

Here $\mathbf{1}$ is the unit tensor, $\mathbf{u}$ is the strain tensor, and $\mathrm{Tr}\mathbf{u}$ denotes its trace. E_1 and E_2 are the deformation potentials for pure dilatation and pure shear, respectively.[21]

In the following we restrict the discussion to the effect of uniaxial tensile stress X in a [110] direction, the particular stress distribution which gives rise to the large piezoresistance in germanium. Only the pure-shear part of the resulting strain will be considered, since the dilatation shifts all valleys and donor states by the same amount and hence does not affect the valley populations.

In n-type germanium there exist four valleys in the [111] directions in momentum space. The shear causes two of the valleys to shift up and the other two to shift down by the same amount ϵ determined by the shear part of (A4) as

$$\epsilon=|\epsilon^{(i)}|=E_2S_{44}X/6. \tag{A5}$$

With this result and denoting $K=\mu_\perp/\mu_{11}$, one obtains in terms of ϵ and ϵ_F the following conductivity changes for the arrangements C and D of Table I:

$$\frac{\Delta\sigma}{\sigma_0}=\left[\pm\frac{K-1}{2K+1}\sinh(\epsilon/kT)+\cosh(\epsilon/kT)\right]\times\exp(\epsilon_F/kT)-1. \tag{A6}$$

The plus sign applies to arrangement C, the minus sign to arrangement D.

In order to calculate ϵ_F, the detailed structure of the lowest lying donor states and their shift due to applied stress have to be known. This problem has been investigated by Kohn and Luttinger[22] and Price.[18] Their results will be briefly summarized below.

In unstrained germanium the four energy minima of the conduction band are completely equivalent.

[20] H. Brooks, in *Advances in Electronics and Electron Physics*, edited by L. Marton (Academic Press, Inc., New York, 1955), Vol. 7, p. 85.

[21] The notation of H. Brooks (reference 20) is adopted here. The relation between his and Herring's notation is $E_1=\Xi_d+1/3\Xi_u$ and $E_2=\Xi_u$.

[22] W. Kohn and J. M. Luttinger, Phys. Rev. **98**, 915 (1955); see also reference 20.

Consequently in the effective-mass approximation the Schrödinger equation has four degenerate solutions for the donor ground state (not counting spin degeneracy). When the crystal is subjected to a specific shear strain **u**, the equivalence of the energy minima is destroyed and the minima shift according to (A4).

In first-order perturbation theory the strain will shift the originally degenerate donor ground states $E_{d0}^{(i)}$ by the same amount $\epsilon_d^{(i)}=\epsilon^{(i)}$ with $\epsilon_d^{(i)}=E_d^{(i)}-E_{d0}^{(i)}$. Figure 11(a) shows the effect of uniaxial stress X applied in the [110] direction on the conduction minima and the donor ground states in the effective-mass approximation. Again only the shear part of the resulting strain has been considered.

Corrections to the effective-mass approximation become largest in the immediate vicinity of the donor atom. The completely symmetrical 1s-like donor state (belonging to the representation A_1 of the tetrahedral group T_d) will be most strongly affected because its wave function is the only one with a large amplitude at the donor nucleus. Because of the attractive potential of the donor nucleus one expects this state to be depressed, whereas the other three 1s-like states remain degenerate in the unstrained crystal and very near the energy obtained from the effective-mass formalism. Following Price, this splitting between the one-fold and the three-fold 1s-like states, called "chemical shift," will be denoted by $4\Delta_c$. Assuming Δ_c to remain unaffected by strain, Price obtained the following shifts of the four 1s-like donor states resulting from the shear part of uniaxial stress in the [110] direction [see Fig. 11(b)]:

$$\begin{aligned}
E_d^{(1)}&=E_{d0}+\Delta_c+\epsilon,\\
E_d^{(2)}&=E_{d0}-\Delta_c+(4\Delta_c^2+\epsilon^2)^{\frac{1}{2}},\\
E_d^{(3)}&=E_{d0}+\Delta_c-\epsilon,\\
E_d^{(4)}&=E_{d0}-\Delta_c-(4\Delta_c^2+\epsilon^2)^{\frac{1}{2}}.
\end{aligned}\tag{A7}$$

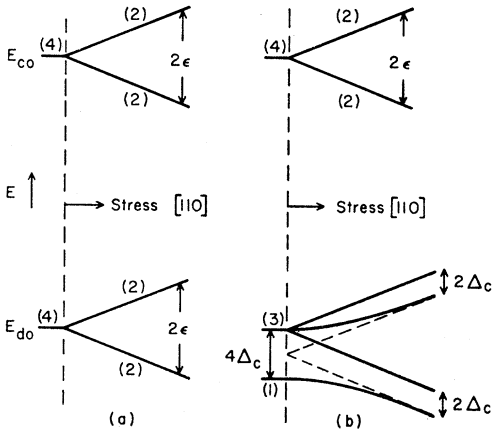

FIG. 11. Shear-induced splitting of the conduction band edge in germanium (upper part) and of the lowest donor-state multiplet (lower part) caused by uniaxial stress in the [110] direction for $\Delta_c=0$ (a) and $\Delta_c\neq 0$ (b). The numbers in parentheses denote degeneracies neglecting the electron spin.

It appears to be a good approximation to set $\epsilon=|\epsilon^{(i)}|$, i.e., equal to the absolute magnitude of the shift of the valleys obtained from (the shear part of) Eq. (A4).

The strain-induced shift, ϵ_F, of the Fermi energy will be calculated for two extreme cases: $\Delta_c=0$ (case I) and $4\Delta_c/kT\gg 1$. In both cases we shall assume donor concentrations low enough so that the donor states are completely localized, i.e., we exclude the possibility of having more than one electron on a given donor.

Case I: $\Delta_c=0$

The Fermi level equation for both cases illustrated in Fig. 11(a) and (b) is

$$\begin{aligned}
&N_c\exp[(E_F-E_{c0})/kT]\cosh(\epsilon/kT)\\
&\quad+N_d/\{1+\exp[(E_{d\,\mathrm{eff}}-E_F)/kT]\}=N_d-N_a,
\end{aligned}\tag{A8}$$

where N_d and N_a are the donor and acceptor concentrations, respectively, N_c is the effective density of states in the conduction band, and E_{c0} is the zero-strain band edge energy. The effective donor-state energy $E_{d\,\mathrm{eff}}$ is given by

$$E_{d\,\mathrm{eff}}=-kT\ln[\textstyle\sum_l g_l\exp(E_d^{(l)}/kT)].\tag{A9}$$

Here g_l denotes the degeneracy of the donor state of energy $E_d^{(l)}$. In the present case [Fig. 11(a)] one obtains

$$E_{d\,\mathrm{eff}}=-kT\ln[8\cosh(\epsilon/kT)].\tag{A10}$$

Substituting (A10) into (A8) yields a Fermi level equation which is identical with that for $\epsilon=0$ except for the substitution[23]

$$\exp(E_{F0}/kT)=\exp(E_F/kT)\cosh(\epsilon/kT).\tag{A11}$$

Since $\exp(E_F/kT)\cosh(\epsilon/kT)$ is a function of quantities independent of ϵ, it follows that the total number of conduction electrons, given by the first term in (A8), remains unchanged by the shift ϵ.

From (A11) one obtains for the shift of the Fermi energy

$$\epsilon_F=-kT\ln\cosh(\epsilon/kT).\tag{A12}$$

Substituting (A12) into (A6) yield the final result

$$\frac{\Delta\sigma}{\sigma_0}=\pm\frac{K-1}{2K+1}\tanh(\epsilon/kT),\tag{A13}$$

with ϵ given by (A5). The plus and minus sign refer, respectively, to arrangements C and D. The first order term in X gives, as expected, the expression of Herring and Adams:

$$\frac{\Delta\sigma}{\sigma_0}=\pm\frac{K-1}{2K+1}\frac{1}{6}\frac{E_2}{kT}S_{44}X.\tag{A14}$$

[23] We follow here an argument which is due to Landsberg; see P. T. Landsberg, Proc. Phys. Soc. (London) **B71**, 69 (1958).

Case II: $4\Delta_c/kT \gg 1$

The level scheme for $\Delta_c \neq 0$ is shown in Fig. 11(b). In order to find ϵ_F one has to solve the Fermi level equation (A8) using the effective donor-state energy (A9) in which $E_d^{(l)}$ is given by (A7). This leads to a complicated expression for ϵ_F which can be solved numerically when the quantities Δ_c and E_2 are known.

One can find, however, a simple expression for the limiting case $4\Delta_c/kT \gg 1$. This condition will always be satisfied at low enough temperatures. The influence of the upper three states of the donor multiplet can then be neglected. At low enough temperatures, i.e., when the total electron concentration $n \ll N_d - N_a$ and $n \ll N_a$, the Fermi energy shifts parallel to the donor ground state energy when stress is applied so that

$$\epsilon_F = 2\Delta_c - (4\Delta_c^2 + \epsilon^2)^{\frac{1}{2}}. \quad \text{(A15)}$$

Substituting (A15) into (A6) yields the final result for the respective conductivity changes:

$$\frac{\Delta\sigma}{\sigma_0} = \left[\pm \frac{K-1}{2K+1} \sinh(\epsilon/kT) + \cosh(\epsilon/kT) \right] \times \exp\{[2\Delta_c - (4\Delta_c^2 + \epsilon^2)^{\frac{1}{2}}]/kT\} - 1, \quad \text{(A16)}$$

with ϵ given by (A5). The plus sign applies to arrangement C, the minus sign to arrangement D.

The case of finite Δ_c differs from the case $\Delta_c = 0$ considered previously in that the total carrier concentration in the conduction band is changed by the stress. This change in n is reflected in a change of the Hall coefficient R:

$$\frac{R - R_0}{R} = 1 - \cosh(\epsilon/kT) \times \exp\{[2\Delta_c - (4\Delta_c^2 + \epsilon^2)]/kT\}. \quad \text{(A17)}$$

In deriving this result, the condition $4\Delta_c \gg kT$ was assumed to hold and the effect of stress on the ratio of Hall mobility to drift mobility was neglected.

PHYSICAL REVIEW VOLUME 115, NUMBER 2 JULY 15, 1959

Electron Damage Thresholds in InSb†

F. H. EISEN AND P. W. BICKEL
Atomics International, Division of North American Aviation, Incorporated, Canoga Park, California

(Received February 18, 1959)

Measurements of carrier removal rate and isochronal recovery in electron-irradiated InSb indicate that displacements are produced at electron energies as low as 240 kev. Two recovery stages have been found and the activation energies for recovery determined. The conductivity recovery in the low-temperature stage was found to be first order.

THE rate at which carriers are removed from the conduction band in InSb by electron bombardment has been measured as a function of energy in an effort to determine the threshold electron energy for the production of atomic displacements. The results are shown in Fig. 1. The irradiation and electrical conductivity measurements, from which the carrier removal rates, $d\bar{n}/dN_e$, were derived, were carried out at liquid nitrogen temperature. The sample was n-type with 1.4×10^{14} carriers/cm$_e$ and a mobility of 3.5×10^5 cm^2/volt sec at liquid nitrogen temperature. The sample thickness was 0.017 cm.

Figure 1 may be separated into an energy region in which $d\bar{n}/dN_e$ changes rapidly with energy and a "tail" region in which $d\bar{n}/dN_e$ changes very slowly with energy, suggesting that two different processes may be responsible for the observed conductivity changes. This possibility was investigated by studying the isochronal recovery of damage produced at different electron energies. Figure 2 shows the data for samples annealed after bombardment at 240 kev and 400 kev. The 240-kev damage recovers in two stages labeled I and II in the diagram. The 400-kev damage recovers entirely in Stage II and the annealing of a sample irradiated at 700 kev shows nearly all the recovery occurring in Stage II (with the rest of the recovery occurring at higher temperatures). The absence of recovery in Stage I after irradiation at these energies may be due to heating of the sample during the irradiation. The conductivity change produced in the 700-kev irradiation is too large to be due to a surface effect, indicating that the damage which recovers in Stage II is due to displacements in the bulk of the sample. Since Stage II recovery is observed at 240 kev, the threshold energy must be less than or equal to 240 kev (this corresponds to a maximum energy transfer of 5.7 ev to an indium atom). The recovery of damage produced by 200-kev electrons was observed to occur entirely in Stage I indicating that the threshold for production of the damage recovering in Stage II is above 200 kev. The nature of the damage recovering in Stage I is not clear at the present; surface effects cannot be ruled out as they were in Stage II.

Isothermal recovery data were obtained after 240-kev and 400-kev irradiations and were combined with the

† This research was supported by the Aeronautical Research Laboratory, Wright Air Development Center.